# 12 Ocular Blood Flow and Metabolism

*Alon Harris, Leslie Abrams Tobe, and Brent Siesky*

## CONTENTS





## INTRODUCTION

The eye offers a unique opportunity to study hemodynamics. It is the only location in the body where capillary blood flow may be observed in humans noninvasively. More than 100 years ago, Wagemann and Salzmann (1892) observed vascular sclerosis in many of their glaucoma patients. Through the years, numerous other researchers have uncovered pieces of the ocular blood flow puzzle: documenting reductions in the capillary beds, sclerosis of nutritional vessels, vascular lesions and degeneration, and other circulatory pathologies in many eye diseases, including glaucoma. A century of observation and circumstantial evidence suggesting a vascular component in the pathogenesis of glaucoma is now supported by direct experimental evidence with specialized measurements of hemodynamic function that are now readily available.

Much evidence suggests that vascular pathologies play an important role in the etiology and progression of open angle glaucoma (OAG), especially given the number of OAG patients with disease progression despite significantly reduced IOP levels. Dozens of prospective studies utilizing a wide spectrum of ocular imaging technologies have reported glaucoma patients have reduced ocular blood flow in the retinal, choroidal, and retrobulbar circulations. It is not yet well established whether this decreased blood flow is related to cause or effect. Some theorize that decreased blood flow causes ischemic insult to the optic disc and retina leading to characteristic glaucomatous progression, and others believe that elevated IOP in glaucoma leads to tissue injury decreasing the need for blood flow to that region. In highly controlled settings, chronic optic nerve ischemia has been shown to induce retinal ganglion cell loss independent of IOP. Direct assessment of ocular hemodynamics may play a role in earlier ophthalmic disease detection, differentiation, and, possibly, new treatment options in the future.

## OCULAR VASCULATURE

### Overview

The ophthalmic artery (OA) supplies both major ocular vascular beds: the retinal and uveal systems. Its major branches include branches to the extraocular muscles, the central retinal artery, and the posterior ciliary arteries (Figure 12.1). The uveal system, which supplies blood to the iris, ciliary body, and choroid, is supplied by one to five posterior ciliary

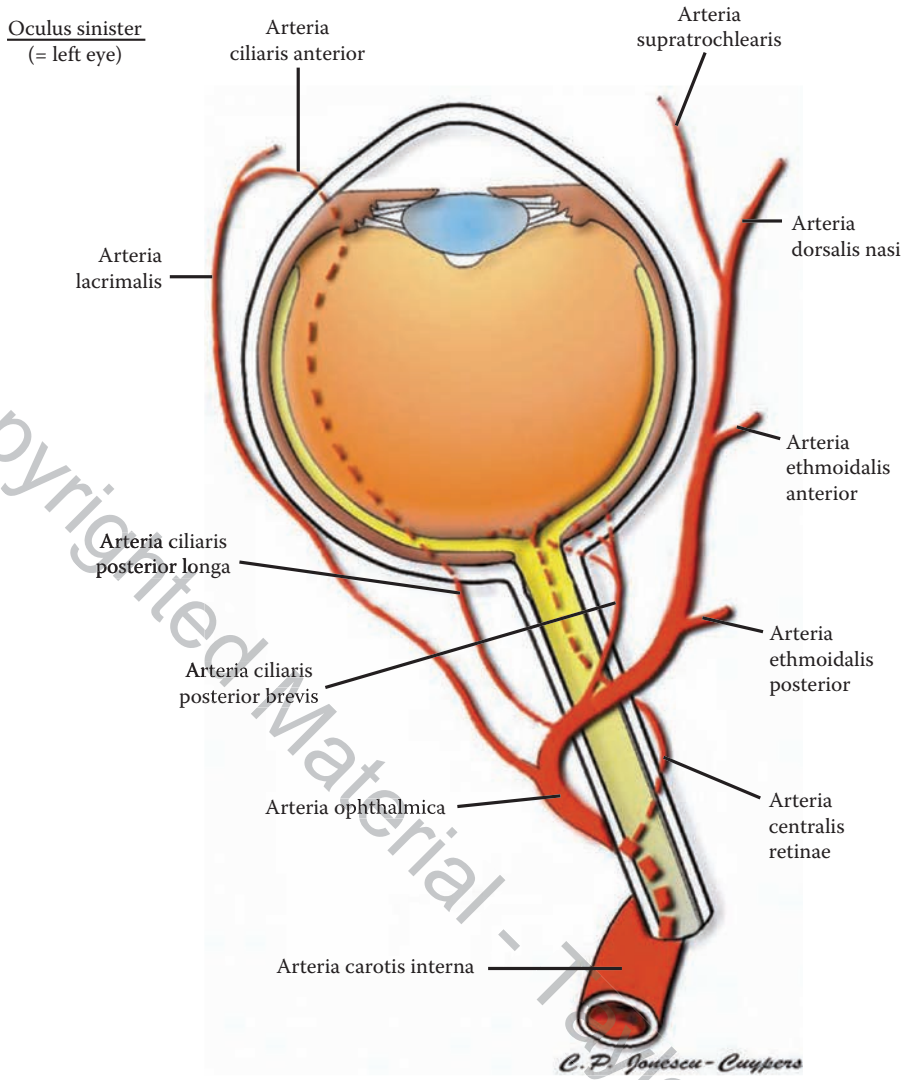


**FIGURE 12.1** Branches originating from the arteria carotis interna.

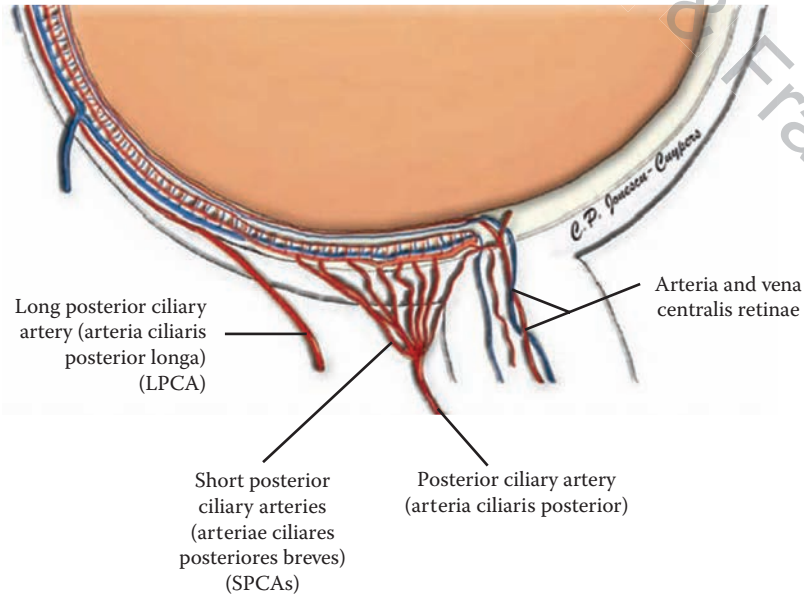


**FIGURE 12.2** Choroidal and retinal vasculature.

arteries (PCA). They emerge from the ophthalmic artery in the posterior orbit. Short posterior ciliary arteries (SPCAs) penetrate the sclera surrounding insertion of the optic nerve (Figure 12.2). These vessels supply the peripapillary choroid as well as the majority of the anterior optic nerve. Some SPCAs course, without branching, through the sclera directly into the choroid; others divide within the sclera to provide branches to both the choroid and the optic nerve. Often, a noncontinuous arterial circle exists within the perineural sclera, the circle of Zinn–Haller. This structure is formed by the convergence of branches from the SPCAs. The circle of Zinn–Haller provides blood for various regions of the anterior optic nerve, the peripapillary choroid, and the pial arterial system.

## Vasculature of the Choroid and Retina

The innermost layer of the choroid, the choriocapillaris, is composed of richly anastomotic, fenestrated capillaries beginning at the optic disc margin (Figure 12.3). The capillaries of the choriocapillaris are separate and distinct from the capillary beds of the anterior optic nerve. The SPCAs supply most of the optic nerve head and the portion of the choriocapillaris posterior to the equator. The choriocapillaris anterior to the equator is supplied by the long posterior ciliary arteries (LPCAs) and the anterior ciliary arteries (ACAs), which are branches of the OA. The LPCAs pierce the sclera and course anteriorly through the suprachoroidal space to branch near the ora serrata. Each LPCA then sends three to five branches posteriorly to supply the choriocapillaris anterior to the equator. The ACAs accompany the rectus muscles anteriorly to supply the major circles of the iris (Figure 12.4). Before reaching the iris, 8–12 branches pass posteriorly through the ciliary muscle to supply the anterior choriocapillaris together with the LPCAs (Figure 12.5). Functional anastomoses between the choriocapillaris anterior and posterior to the equator have not been demonstrated, representing a peripheral choroidal watershed zone.

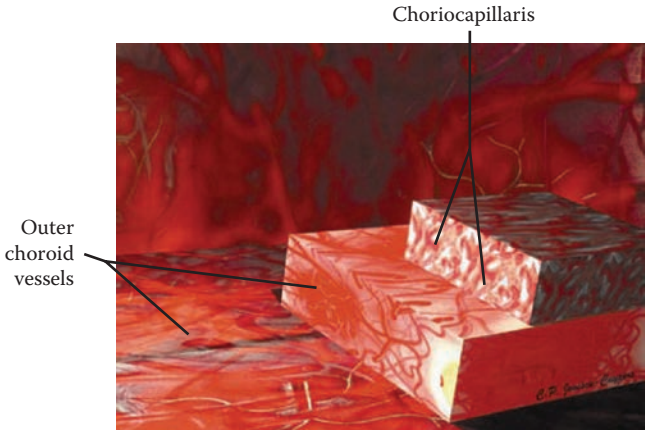


**FIGURE 12.3** Cross section of choroidal vascular bed.

Venous drainage from the choriocapillaris is mainly through the vortex vein system. Minor drainage occurs through the ciliary body via the anterior ciliary veins. The vortex veins drain into the inferior (IOV) and superior (SOV) ophthalmic veins (Figure 12.6).

The retinal system is supplied by the central retinal artery (CRA) and sustains the inner retina. The CRA, itself a branch of the ophthalmic artery, penetrates the optic nerve approximately 12 mm behind the globe. The CRA courses adjacent to the central retinal vein through the center of the optic nerve, then emerges from the optic nerve within the globe, where it branches into four major vessels.

The anterior optic nerve may be divided into four anatomic regions: the superficial nerve fiber layer, the prelaminar region, the lamina cribrosa, and the retrolaminar region (Figure 12.7). The superficial nerve fiber layer, the anteriormost region, is continuous with the nerve fiber layer of the retina and is the only nerve head structure visible by fundus examination (Figure 12.7, yellow shaded). It is supplied by retinal arterioles arising from the branches of retinal arteries.

Immediately posterior to the nerve fiber layer is the prelaminar region, which lies adjacent to the peripapillary choroids (Figure 12.7, red shaded). The prelaminar region is supplied primarily by branches of the SPCAs and by branches of the circle of Zinn–Haller although some investigators have observed a vascular contribution to the prelaminar region from peripapillary choroidal arterioles. The direct arterial supply to the prelaminar region arising from the choroidal vasculature is minimal and is limited to small arterioles.

More posteriorly, the laminar region is continuous with the sclera and is composed of the lamina cribrosa (Figure 12.7, green shaded). Like the prelaminar region, the lamina cribrosa also receives its blood supply from branches of the SPCAs and branches of the circle of Zinn–Haller. Larger vessels of the peripapillary choroid may contribute occasional small arterioles to the lamina cribrosa region.

Finally, the retrolaminar region lies posterior to the lamina cribrosa and is surrounded by the meninges of the central nervous system (Figure 12.7, blue shaded). The retrolaminar region has two blood supplies: the CRA and the pial system. The pial system originates at the circle of Zinn–Haller and may also be fed directly by the SPCAs. The CRA may provide several small intraneural branches in the retrolaminar region. Some of these branches anastomose with the pial system.

There is a marked inter-individual variation in the vascular patterns of the anterior optic nerve, peripapillary retina, and posterior choroid, predominately in the arterial supply. Varying numbers of branches have been found in the posterior ciliary arteries, the SPCAs, the number of branches from the LPCAs, and the number of branches from the ACAs.

The most recent evidence suggests that glaucoma affects the photoreceptors and the horizontal cells as well as the retinal ganglion cells. The retinal ganglion cells are nourished

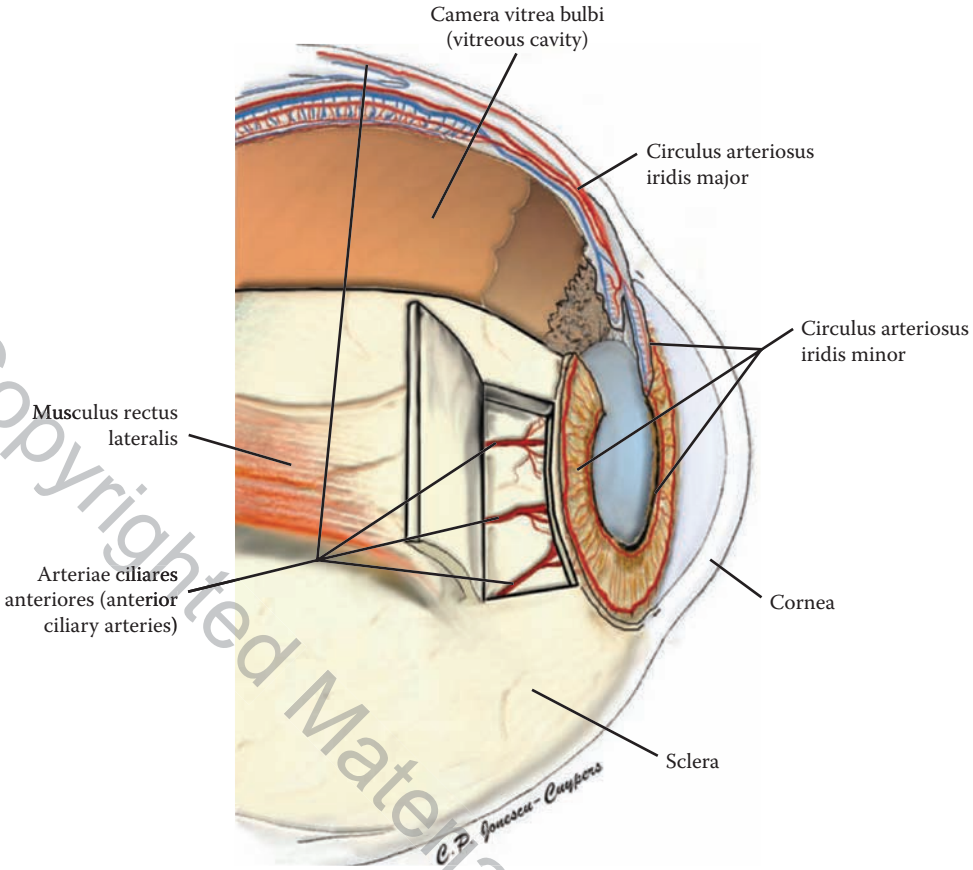


FIGURE 12.4 Anterior segment.

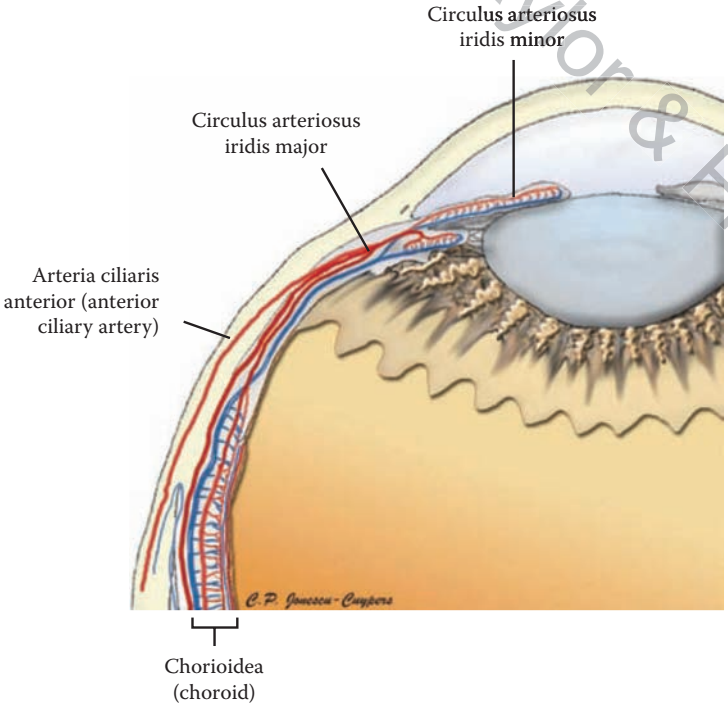


FIGURE 12.5 Anterior vessels.

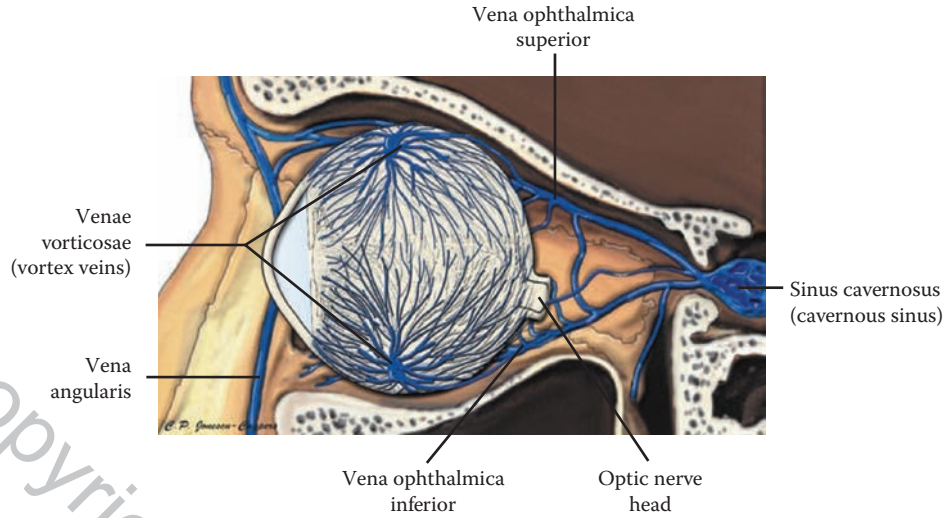


**FIGURE 12.6** Venous drainage of the orbit and globe.

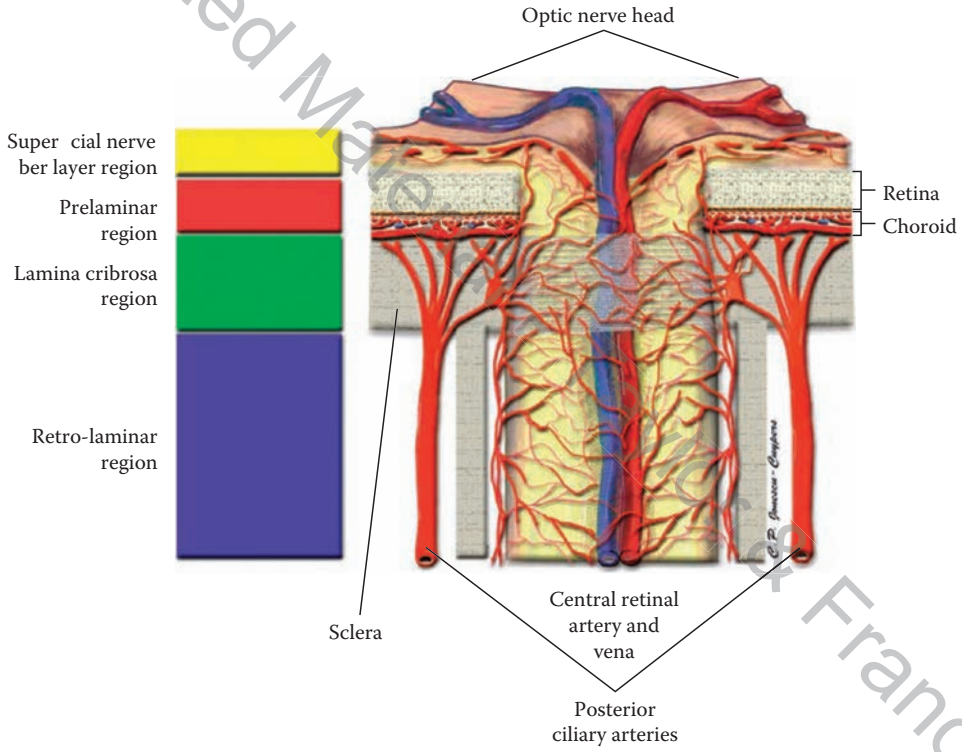


**FIGURE 12.7** Optic nerve head vasculature. (Reprinted from *Atlas of Ocular Blood Flow: Vascular Anatomy, Pathophysiology, and Metabolism,* Harris A et al., Copyright 2003, with permission from Elsevier.)



by the retinal circulation, and the photoreceptors receive their blood supply from the underlying choroid. Therefore, to define how enhanced blood flow improves visual function, it is essential to evaluate blood flow to the retina and choroid.

## OCULAR PERFUSION PRESSURE

Perfusion pressure in the eye is defined as the difference between arterial blood pressure and IOP. Ocular perfusion pressure (OPP) can be calculated with the following equations, including OPP, diastolic (DOPP), and systolic (SOPP) specific perfusion pressures:

$$\text{OPP} = (\text{two thirds mean arterial pressure} - \text{IOP})$$

$$\text{DOPP} = (\text{diastolic blood pressure} - \text{IOP})$$

$$\text{SOPP} = (\text{systolic blood pressure} - \text{IOP})$$

Ocular blood flow (OBF) in healthy individuals is autoregulated to maintain constant flow to sensitive ocular tissues despite fluctuating blood pressure and IOP. In glaucoma patients, however, it is thought that defective autoregulation may result in ischemic damage and possible reperfusion injury. Given known diurnal variation in blood pressure and IOP, it is possible that chronic intermittent ocular ischemia damages retinal ganglion cells during periods of high IOP and/or low systemic blood pressure as expressed in ocular perfusion pressures. Numerous population-based studies have linked low ocular perfusion pressures with OAG prevalence, incidence, and progression. A better understanding of the effect of OPP on delivery of blood and oxygen to the ocular tissues in patients with OAG may provide the missing link in understanding glaucoma risk.

## TECHNIQUES FOR EXAMINING OCULAR BLOOD FLOW

Technological revolutions in medical science have enabled clinicians and researchers to better measure OBF. In the past few decades, ocular hemodynamic assessment has evolved from a subjective description of visible vessels to direct quantitative measurement of blood flow parameters. The most important limitation in directly assessing OBF in humans is a lack of a sufficient gold standard for the measurement of OBF. The various methods currently in use all have inherent limitations and measure different aspects of OBF. In addition, the assessment of OBF requires highly skilled experienced technicians and is expensive, and availability of imaging technologies is greatly limited.

While limitations exist, accurate and reproducible data from qualified research centers is still possible. Each ocular blood flow assessment methodology provides some degree of insight into the various ocular vascular beds. Below is a summary of the existing methodologies for assessing ocular blood flow in humans.

## COLOR DOPPLER IMAGING

Color Doppler imaging (CDI) is the most commonly utilized and established methodology to measure aspects of the ocular circulation. This technology is used in many different parts of the body, such as the carotid arteries. Thus, its application in the eye is based upon easily understood principles. The technology also has the advantage of being available in most hospital settings.

Ultrasound technology uses sound waves to locate structures in the body. By timing the delay between sound transmission and echo, ultrasound can measure the depth and location of an anatomic structure. For example, an A-scan ultrasound determines axial length by measuring the time between transmission of a sound wave into the eye and the returning echo from the back of the eye. By sweeping the A-scan in a line through the eye, a map of structural locations through a slice is obtained. This is commonly known as B-scan ultrasound and has been used to produce grayscale images of ophthalmic structures. CDI is based on B-scan technology with an additional processing step.

In CDI (Figure 12.8), the frequency of the returning B-scan sound waves are analyzed, and when a wave is reflected by a moving source, such as flowing blood, it is Doppler-shifted to a different frequency. The amount of the shift is described by the Doppler equation (Shift = $2V_{Blood}Cos\theta$/Wavelength), where Wavelength is the wavelength of the incident sound wave, and Cosθ is the cosine of the angle between the blood velocity vector and the incident sound wave vector. Doppler-shifted sound is displayed using color-coded pixels within the grayscale image. Red pixels represent movement toward the CDI probe, and blue represents movement away from the probe. Samples of Doppler shifts may be collected from specified vessels within the image in real time during the cardiac cycle. Data may be obtained from the resulting velocity waveform. The peak systolic velocity (PSV) is located by the ultrasonographer and is equal to the greatest observable flow velocity obtained during systole. The end-diastolic blood flow velocity (EDV) can also be located by the ultrasonographer (Figure 12.9). Using both of these measurements, Pourcelot's resistive index (RI) may be computed as RI = PSV – EDV/PSV. RI is an indication of the resistance to flow in the vasculature distal to the point of measurement.

CDI is used to measure blood flow velocities in the OA, CRA, and SPCAs. Due to the large difference between the OA and the smaller CRA and SPCAs, the system settings are changed to appropriate ranges of depth and velocity. The waveforms of the various vessels provide additional information. The dicrotic notch is clearly evident in the OA waveform while still evident yet less pronounced in the CRA and missing from the SPCA. The appearance of waveforms may

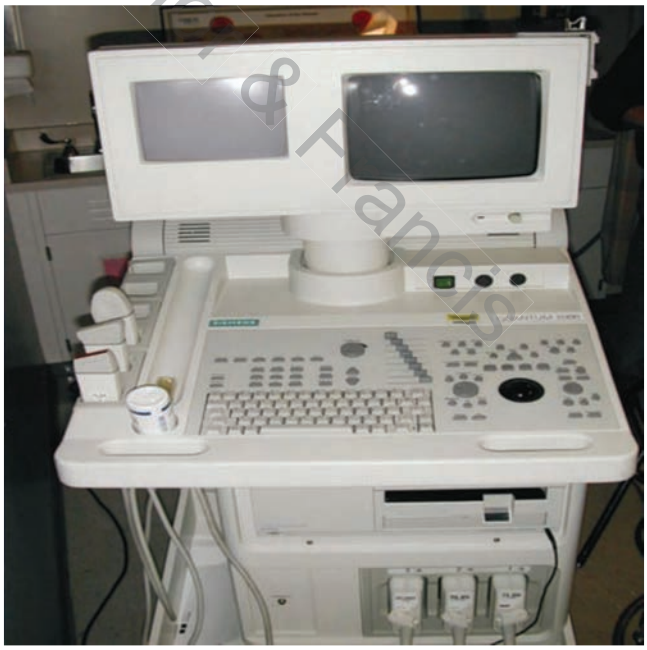

**FIGURE 12.8** Color Doppler imaging ultrasound machine. (Courtesy of Siemens Quantum 2000, Siemens Ultrasound, Isaquaah, WA.)

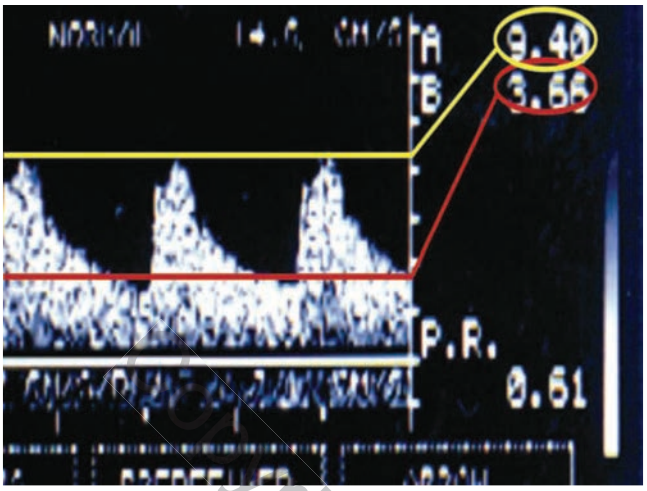


FIGURE 12.9 Peak systolic velocity and end diastolic velocity. These are marked by the ultrasonographer and resistive index is then calculated from these values.

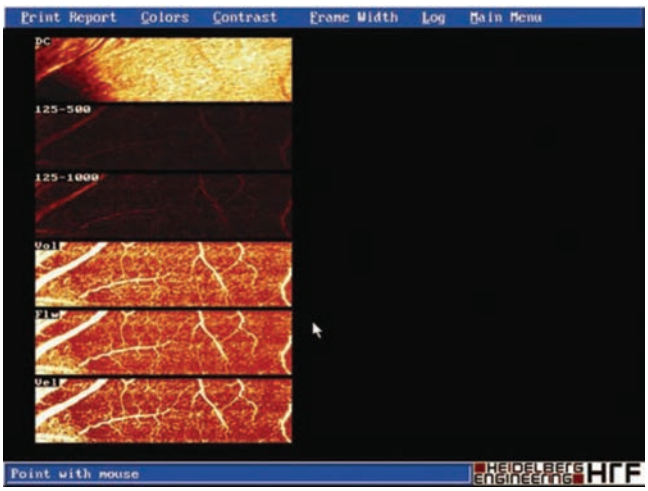


FIGURE 12.10 Map of retinal blood flow produced by Heidelberg Retinal Flowmeter (HRF).

also provide insight into the condition of the patient's ocular vascular health.

CDI is safe, validated, and noninvasive and produces reliable information about the retrobulbar circulation. It does not require clear optical media and can thus be performed in the presence of many ophthalmic diseases. However, the technique is limited as CDI is expensive and requires a skilled technician for reproducible measurements. Additionally, most CDI applications do not have an ability to determine blood vessel diameter, thereby producing only blood flow velocities.

## LASER DOPPLER TECHNIQUES

### Laser Doppler Flowmeter

Laser Doppler technology has also been employed to quantify ophthalmic blood flow. The Laser Doppler flowmeter (LDF) is a laser Doppler device consisting of a modified fundus camera and computer. It is designed to measure volumetric flow in the capillary beds of retinal and choroidal tissue. It works by positioning a laser onto a location of interest and a detector over the illumination point. Significant limitations include nonuniformity in analysis methods, requirement of clear optical media, and good fixation, and the source of measured Doppler shifts may be both the retinal and choroidal vasculature. The complexity and difficulty of operation and the nonuniformity in analysis methods have kept the Riva LDF from gaining popularity clinically or in research.

### Confocal Scanning Laser Doppler Flowmetry

Heidelberg Engineering of Heidelberg, Germany, produces a scanning version of the LDF to assess retinal capillary blood flow with coefficients of reliability near 0.85. The Heidelberg retinal flowmeter (HRF) scans the fundus, creating a map of retinal blood flow (Figure 12.10). Three flow parameters are displayed: volume, flow, and velocity. Values are in arbitrary units with absolute values depending on the optical scattering characteristics of individual eyes. Unlike the stationary laser point of the LDF, the HRF laser quickly scans the fundus. Each scan line is divided into 256 individual points. Doppler shifts from each point are considered independently. Scattered light from each point is quantified as with LDF; however, only scattered light from the point of illumination is analyzed by the HRF. Because separation of the incident beam and detection point (as used in the LDF) increases penetration of the measurement, HRF measurements will tend to be concentrated on surface vasculature. Further, the system is confocal, with a focal plane thickness of 400 μm, therefore eliminating the contribution of deeper tissue to the measurement.

Utilizing the high spatial resolution of the HRF, an analysis technique has been developed that quantifies capillary density in concert with quantification of blood flow within those same capillaries. Using the HRF, flow measurements of living tissue are obtained at a resolution sufficient to discern capillaries and the avascular tissue between them. The percentage of tissue between capillaries is calculated as a percentage of total tissue volume. Individual flow measurements within those same capillaries are described in a histogram (Figure 12.11). Cumulative percentage landmarks are then used to describe the distribution of capillary flow. This provides a complete assessment of the hemodynamics in a given tissue. To its advantage, the HRF measures volumetric flow although in arbitrary units. HRF systems are no longer commercially available.

### Canon Laser Blood Flowmeter

The Canon laser blood flowmeter (CLBF) is the only hemodynamic assessment device capable of measuring volumetric blood flow in absolute units in larger vessels. The CLBF is a Windows-based flowmeter that uses two lasers to simultaneously measure blood velocity and vessel diameter. Blood flow

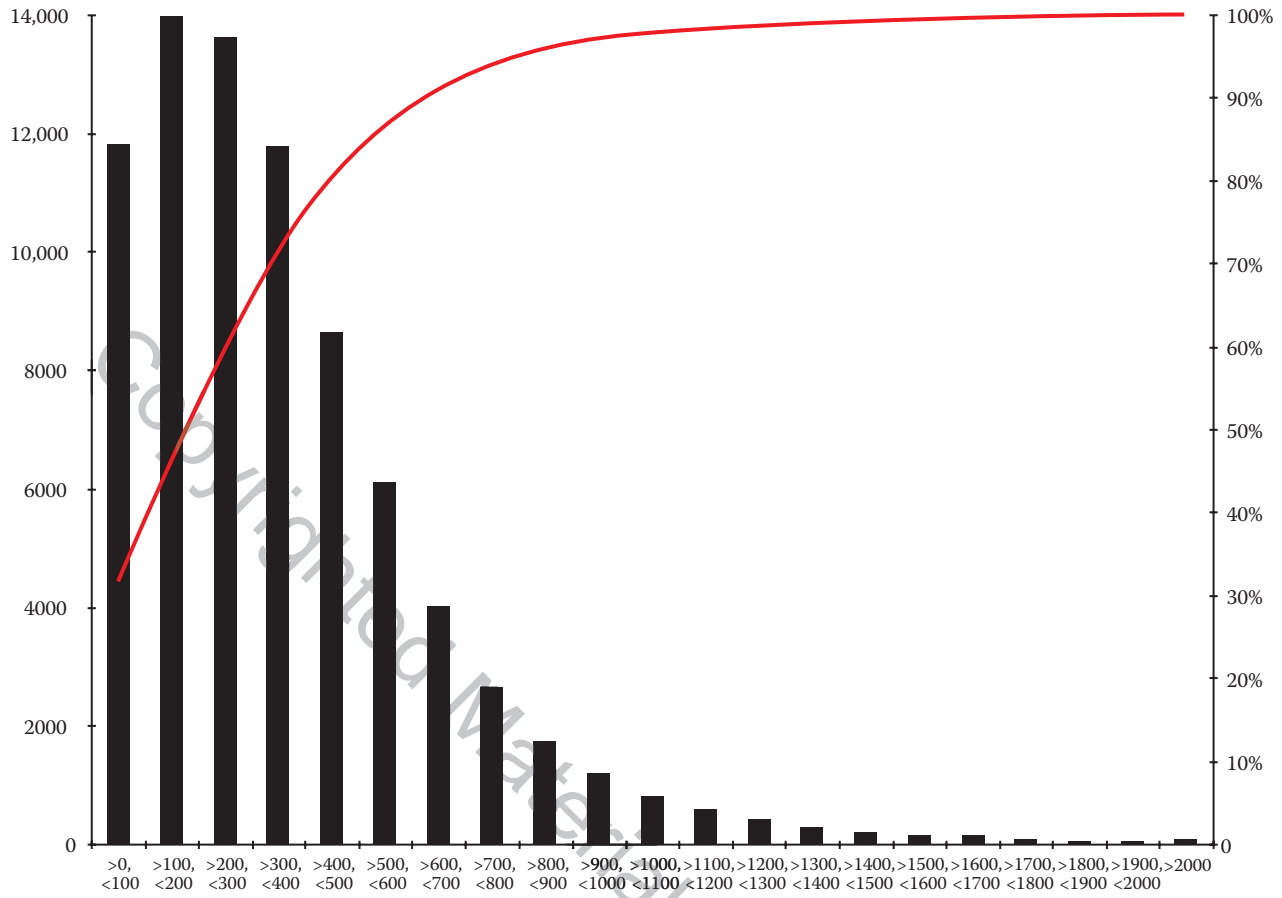


FIGURE 12.11 Individual flow measurements from within the capillaries as measured using the HRF.

is calculated from these two measurements. Used in a manner similar to a fundus camera, the CLBF provides an image of the fundus, from which the technician can identify a large retinal artery or vein and measure blood flow velocity based on the Doppler principle (Figure 12.12). Like the HRF, the CLBF is no longer commercially available.

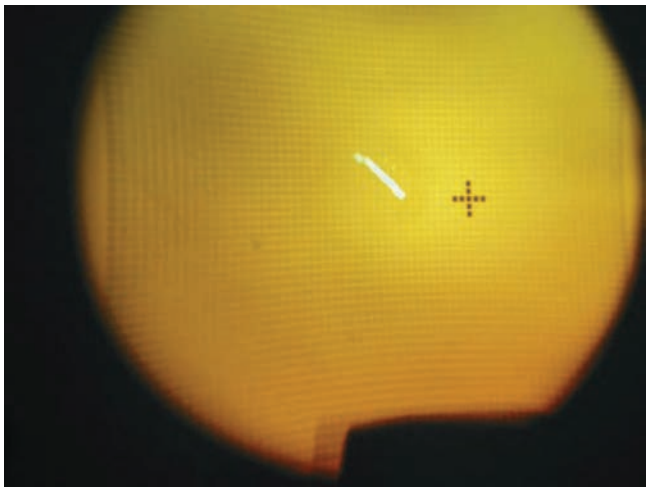

FIGURE 12.12 Image of fundus viewed through the CLBF.

## PULSATILE OCULAR BLOOD FLOW

The pulsatile ocular blood flow (POBF) device (OBF Labs Ltd., UK, Figure 12.13) is a pneumotonometer that measures IOP and derived ocular pulse amplitudes (OPA) in real time. It is based on the principle that blood surges into

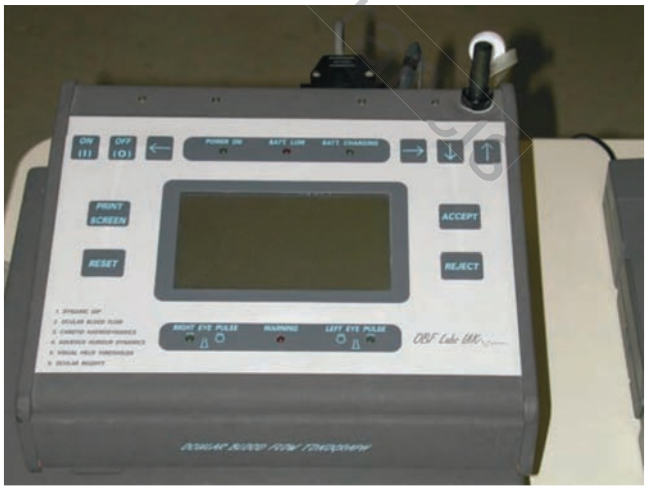


FIGURE 12.13 Pubsatile ocular blood flow device. (Courtesy of OBF Labs UK, Ltd., Malmesbury, Wiltshire, England.)

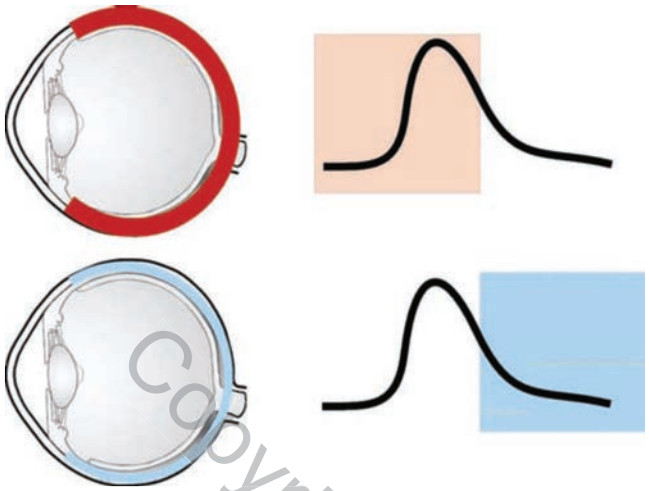

**FIGURE 12.14** Representation of the principle of pulsatile ocular blood flow measurements. Blood volume in the eye increases with the systolic pulse and decreased during diastole.

the blood vessels of the eye during systole and continues to flow more gradually during diastole, creating an ocular pulse amplitude, which is then converted to a calculation of POBF (Figure 12.14). The advantage of this system is that it is inexpensive; however, the obvious disadvantage is that POBF is not a direct measurement of blood flow.

## OCULO-OPHTHALMODYNAMAMOGRAPHY

The oculo-ophthalmodynamamograph device is a pneumotonometer that measures IOP and calculates perfusion pressure in real time (Figure 12.15). During the measurement, IOP is increased, and thus flow ceases within each of the vascular beds within the globe. When blood flow ceases within a vascular bed, its contribution to the IOP waveform measured by the pneumotonometer disappears, which allows direct quantification of the perfusion pressure within the uveal and retinal beds. Like POBF, this is not a direct measurement of OBF.

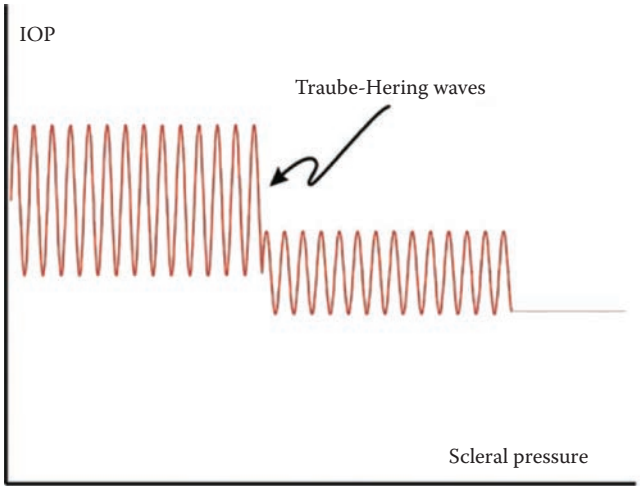


**FIGURE 12.15** Waveform produced by the oculo-ophthalmodynamamograph (OODG). This measures IOP in real time.

## ANGIOGRAPHY

The scanning laser ophthalmoscope (SLO) is a camera system that allows for the quantification of blood flow parameters in the retinal and choroidal tissues. Ophthalmic angiography dates back to 1961 when Novotny and Alvis first described the method. The SLO can be used for fluorescein (FA) or indocyanine green (ICG) angiography. Many different parameters of velocity and blood speed are recorded during these dye injections and digitized for analysis.

For each point of the image, light is focused on a point on the fundus. Light reflected from this point is quantified by a photodetector. Confocal systems create sharp images by blocking scattered light from the image. Only light from the point of interest is focused to a point at the aperture. By recording fluorescein and indocyanine green angiograms, the SLO systems provide valuable data concerning the movement of blood through the retinal and choroidal vasculature; however, measurement of volumetric blood flow by angiography is currently impossible.

Macro and micro retinal hemodynamics evaluated by the SLO FA system are usually quantified by arteriovenous passage (AVP) time and capillary transit velocities (CTV). AVP time is analogous to mean circulation time and is equal to the difference in the time of dye arrival in a retinal artery and corresponding retinal vein. Reductions in AVP have been observed in patients with glaucoma. The SLO's high temporal resolution also permits visualization of hyper- and hypo-fluorescent segments in the perimacular and peripapillary capillary circulation, demonstrating optic disc capillary dropout correlating with visual field loss and morphometric damage in patients with glaucoma.

SLO with ICG dye can be utilized to measure choroidal blood flow as the near-infrared light penetrates the pigmented layers of the fundus while ICG has a high affinity for plasma proteins. As a result, ICG diffuses slowly out of the fenestrated choriocapillaris, which allows higher resolution of choroidal vasculature. Data from glaucomatous eyes suggest regions of slow choroidal filling and sluggish movement of blood into and out of the choroid.

The greatest limitation of SLO imaging is that the technique is highly invasive, including pupil dilation and dye injections into the vasculature. Due to the invasiveness of the technique, it has become less utilized in recent years.

## INTERFEROMETRY

Interferometry is a technique used to directly measure the pulsation of blood flow of the fundus relative to the cornea. The technique is based on the interference pattern formed by two sources of light: one reflected from the fundus and one reflected from the cornea. The two beams are created from a single laser beam passing through the center of the eye. The single beam is partially reflected by the cornea and also partially reflected by the retina (Figure 12.16). Distance change

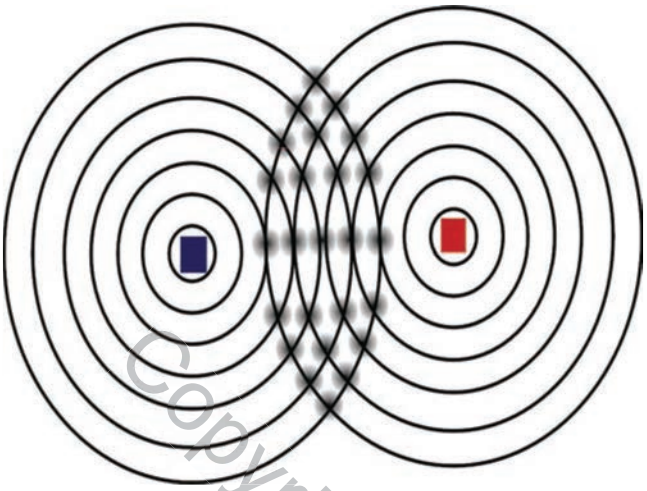

FIGURE 12.16 Diagrammatic representation of the principle of interferometry.

between the cornea and retina as it occurs, for instance, due to the rhythmic filling of blood vessels during the cardiac cycle, is seen as a change in interference order. The maximum distance change between cornea and retina is called fundus pulsation amplitude (FPA) and provides information on the pulsatile component of ocular blood flow.

The technique is noninvasive; however, it requires clear optic media and analysis methods are nonstandard with no commercial availability. Additionally, the ratio of pulsatile to total ocular blood flow and the relative contributions of different vascular beds is unknown.

## RETINAL VESSEL ANALYZER

The Retinal Vessel Analyzer (RVA) (Jena) produces real-time measurements of large retinal vessels with a spatial resolution of less than 1 μm and physical resolution of approximately 17 μm per pixel, accomplished through a statistical process. RVA systems monitor the pulsation of retinal vessels throughout the cardiac cycle assessing vascular tone by performing a rapid series of vessel diameter measurements and maintaining a floating average over time. The RVA provides information on vascular tone but does not measure blood flow and is limited in the size of the vessels it can accurately assess. It also may lack sensitivity to changes in peripheral vascular tone and altered blood rheology.

## BLUE FIELD ENTOPIC TECHNIQUES

Blue field entopic techniques are founded on the blue field entoptic phenomenon. This phenomenon is based on the observation of leukocytes flowing through the subject's own retinal macular vasculature. These methods can be used for a noninvasive, subjective evaluation of perimacular hemodynamic parameters but are not often utilized because the technique is based on the assumption that macular capillaries have a fixed diameter while, in reality, large variations between patients exist. Also, data is limited to the perifoveal anatomical region and depends on the patient's cooperation and perception.

## LASER SPECKLE FLOWMETRY

Laser speckle flowmetry is a noninvasive technique that uses the interference pattern created by light reflected from the fundus and anterior surface of the cornea to measure the amplitude of fundus pulsation with the cardiac cycle (Figure 12.17). The laser speckle method follows time change in the tissue velocity at the same site of the same eye at various intervals. The outcome variables of this method are the square blur ratio (SBR) or normalized blur (NB) values of the selected region in arbitrary units. The technique has produced reproducible measurements, but the two greatest disadvantages of the technique are that the technology is not commercially available, and the meaning of the raw normalized blur measurement is not clearly understood.

## FOURIER-DOMAIN OPTICAL COHERENCE TOMOGRAPHY

The Fourier-domain (FD) optical coherence tomography (OCT) (RTVue100, Optovue Inc., Fremont, CA) is the newest ocular blood flow imaging technology to emerge. It combines OCT structural measurements with the ability to measure total retinal blood flow with Doppler functionality in a single device. The development of this application therefore offers great hope in expanding the availability of retinal blood flow assessment to everyday clinical practice.

Retinal blood flow scans (Figure 12.18) transect all retinal branch arteries and veins emerging from the optic nerve head (ONH), providing the basis for total retinal blood flow measurement (Figure 12.19). Five Doppler OCT scans are taken while three-dimensional (3D) volume scans of the ONH are acquired. The Doppler and the 3D disk data are analyzed, and intensity data from the circular scans are displayed simultaneously. The software automatically detects the

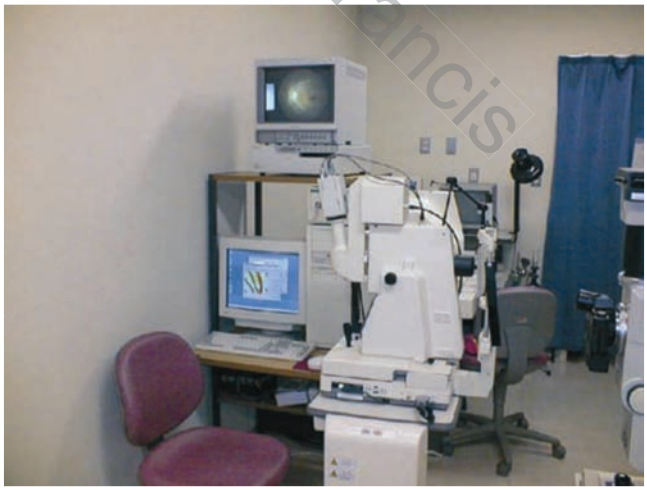

FIGURE 12.17 Laser speckle flowmeter.

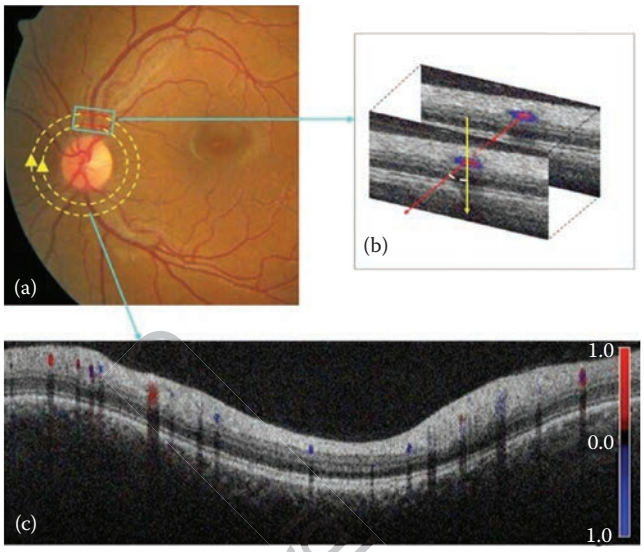


**FIGURE 12.18** Fourier-Domain Optical Coherence Tomography. (a) Fundus photograph showing the double circular pattern of the optical coherence tomography (OCT) beam scanning across retinal blood vessels emerging from the optic disc. (b) The relative position of a blood vessel in the two OCT cross sections is used to calculate the Doppler angle θ between the beam and the blood vessel. (c) Color Doppler OCT image showing the unfolded cross section from a circular scan.

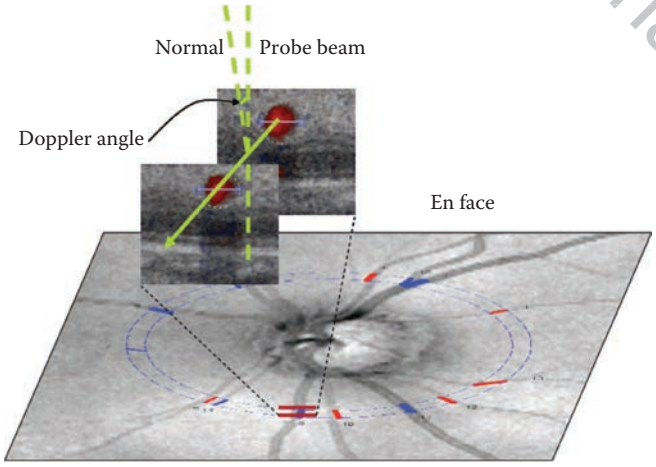


**FIGURE 12.19** Fourier-domain Optical Coherence Tomography. OCT image of double circle scan and 3D scan plus disc photograph are input DOCTORC for grading. (From Tan O et al., Dual Angle Scan Protocol for Doppler Optical Coherence Tomography of Retinal Blood Flow, ARVO 2011, Fort Lauderdale.)

location of the vessels on each frame and matches the same vessel across all frames. With the vessel displayed in both the Doppler OCT phase as well as the standard intensity/reflectivity scan, the grader verifies each vessel's location and the accuracy of the match (on both circular scans) for each of five repeated Doppler OCT acquisitions. The grader corrects the vessel location and the match if necessary. After manual correction, vessel angle and flow calculations are performed automatically and the results are exported. For each of the five repeated Doppler scans, the vessel positions should correspond with the vessel pattern from the en face summation/projection image from the 3D disk scan. Scans with mismatch of >10% of vessels and frames showing evidence of eye movement are flagged as problem cases by the graders.

A pilot study by Harris et al. (2010) looked at measurements of blood flow by FD-OCT in glaucoma patients. They found that patients with OAG had lower total retinal blood flow by 23.9% compared to healthy controls as measured by FD-OCT. They also found a statistically significant correlation between CDI-assessed ophthalmic artery PSV and nasal short posterior ciliary arteries EDV and FD-OCT blood flow. A study by Konduru et al. (2012) found that patients with glaucoma had lower retinal blood flow compared to normal eyes as measured with FD-OCT. This same study also found that the decrease in blood flow was highly correlated with the severity of visual field loss. This suggests that patients with OAG have lower total retinal blood flow than healthy controls as measured with FD-OCT.

The development of FD-OCT blood flow methodologies is of great promise to the progress of clinically available standardized ocular blood flow assessments. More research is required before the full capabilities of FD-OCT blood flow assessment are known.

## RETINAL OXIMETRY

The measurement of ocular blood flow is often used as a surrogate assessment of the metabolic status of the retina. The direct measurement of retinal tissue oxygenation, therefore, may help reveal the true impact of ischemia on retinal photoreceptor ganglion cells.

Current methods aimed at measuring retinal oxygenation involve photographic retinal oximetry. Retinal oximetry involves a modified fundus camera or similar device and applying algorithms to record oxygen levels within ocular tissues. Measuring the oxygenated hemoglobin as a percentage of total hemoglobin using optical spectral techniques is not a new concept. The first oximetry paper on human retinal vessels was published in 1959 by Hickam, Sieker, and Frayser. They used photographic film to record images of vessels on the optic disc, resulting in detailed studies during the next decade of the retinal venous saturation, arterio-venous saturation difference, and changes brought about by vasoactive drugs. This work was the first to show that the vessel oxygen saturation is proportionate to a ratio of vessel optical densities at two measurement wavelengths.

In 1999, Beach et al. reported a digital imaging method for measuring saturation in retinal vessels. Digital spectral retinal oximetry is a noninvasive oxygen measurement based on optical methods, which detect the ratio of oxygenated (red) to deoxygenated (blue) blood (Figure 12.20). As evidenced by their different colors, oxygenated and deoxygenated hemoglobin possess different optical characteristics. Measurement involves passing two wavelengths of light through (or bouncing them off) the tissue of interest. The ratio between the resulting light intensities represents oxygen tension (Figures 12.21 and 12.22). In 2006, Hardarson et al. added extensive computer

FIGURE 12.20 Digital spectral retinal oximeter.

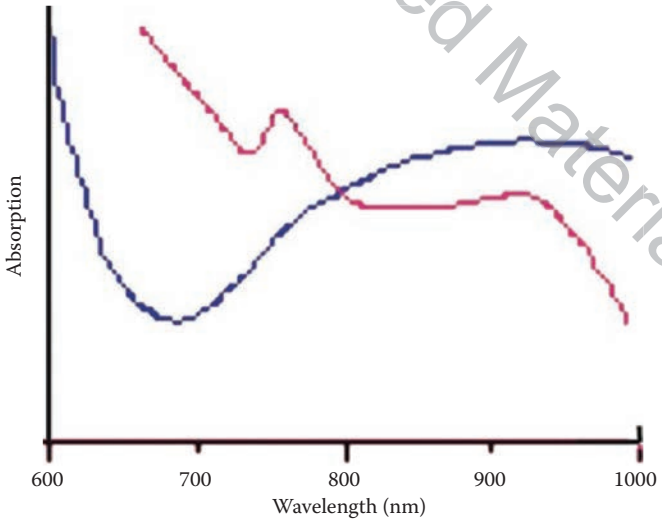


FIGURE 12.21 Plot showing absorption at various wavelengths from the digital spectral retinal oximeter.

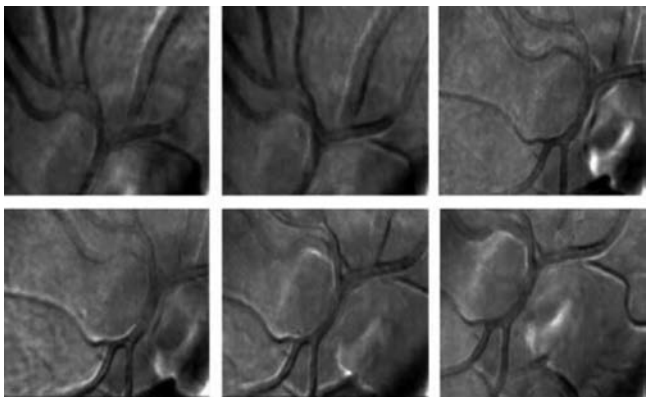

FIGURE 12.22 Images obtained with the digital spectral retinal oximeter at differing wavelengths.

automation that enabled saturation maps of the retinal vessels to be produced automatically after taking the dual wavelength images.

The Oxymap retinal vessel oximeter (Oxymap ehf, Reykjavik, Iceland) is a system that attempts to determine artery and vein saturations over a 50-degree field captured in a single set of oxygen-sensitive and oxygen-insensitive images (Figure 12.23). Optical density ratios (ODR), which are proportional to oxygen saturation, are found from reflected light measured within and outside the vessels in each of the images, according to the following expressions:

$$OD_{570} = \log(I_{outside,570}/I_{inside,570})$$

$$OD_{600} = \log(I_{outside,600}/I_{inside,600})$$

$$ODR = OD_{600}/OD_{570}$$

$$O2Sat \propto A * ODR + B$$

where A and B are calibration coefficients that have been chosen to adjust the ODR to an accepted literature value for retinal arteries. A saturation map of the vessels is automatically displayed to the photographer after the image is taken (Figure 12.24). Statistical information from single vessel segments is found interactively from vascular segments. Other companies have also produced systems for retinal oximetry, including an imaging system from Imedos in Jena, Germany, that is based on the dual wavelength method. This system has the advantage of being simple in concept. It requires just a fundus camera and a special optical filter and can measure retinal oxygenation in the full field of the fundus camera.

Studies have recently begun to emerge that examine retinal oxygen metabolism and glaucoma. One study in particular by Olafsdottir et al. (2011) found larger glaucomatous visual field defects were associated with increased oxygen saturation in venules and decreased arteriovenous difference in retinal oxygen saturation as measured by spectrophotometric retinal oximetery, possibly attributable to tissue loss. More larger, population-based studies are needed to truly assess the relationship between retinal metabolism and glaucoma.

Another relevant application of oximetry is that of magnetic resonance oximetry. Magnetic resonance oximetry measurements are based on the principle that oxygen is a paramagnetic compound that directly influences the spin-lattice relaxation rate (1/T1). The T1 relaxation time is a function of many factors besides local oxygen tension. To eliminate other factors that can affect the observed T1, such as flow, measurements are limited to the posterior vitreous near the retina. Oxygenation of the posterior vitreous near the retina is used as a measure of inner retinal oxygenation (Figure 12.25).

New and emerging metabolic assessment tools may help to specifically reveal how reductions in ocular blood flow and ocular tissue hypoxia are related. As with any developing technologies, a better understanding of the complex optical environment in the ocular fundus is needed to bring the technique forward to where it can be used as a reliable method

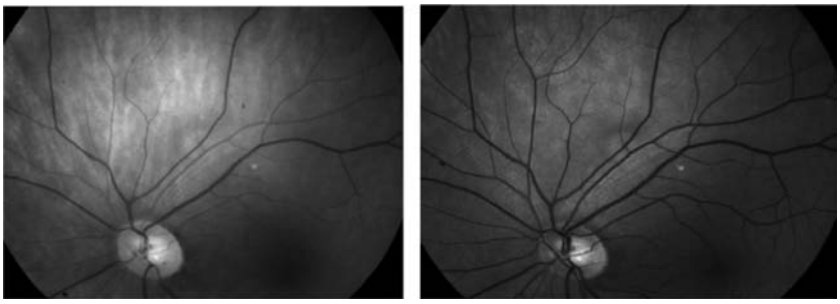

FIGURE 12.23 Simultaneously recorded images of the human retinal vessels using a single flash. Left: oxygen-sensitive image at 600 nm. Right: oxygen-insensitive image at 570 nm.

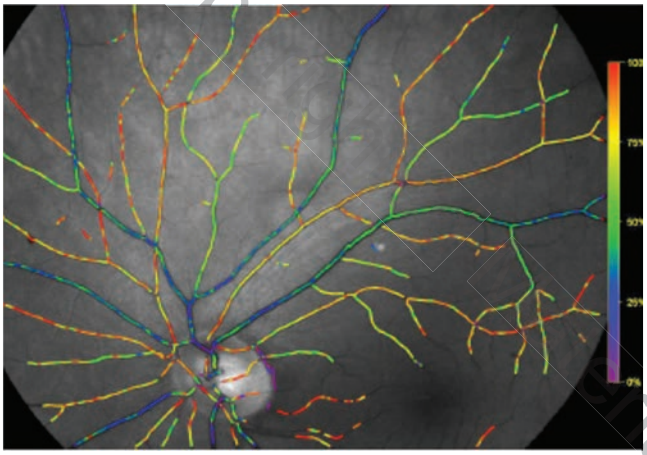

FIGURE 12.24 Color overlay of oxygen saturation in the retinal vessels in retinal oximetry.


FIGURE 12.25 Image and digital representation of the inner retina using magnetic resonance oximetry.

for understanding differences in oxygen utilization in normal and disease populations. The greatest current limitation of retinal photographic oximetry is that it has not been sufficiently validated. Further, the assessment of metabolism is limited to retinal tissues with the current devices and may not reflect oxygen levels in the optic nerve head. Further research is required to understand how tissue oxygenation levels measured by photographic oximetry may be involved in ocular pathologies, including glaucoma.

## CONCLUSIONS

Glaucoma is a comprehensive term for a heterogeneous disease comprised of multiple intertwining etiologies, including elevated IOP and ocular blood flow disturbances. Aberrations in ocular blood flow have become increasingly implicated in OAG disease pathology in recent years due to advances in imaging technologies as described above and ever increasing data from clinical studies.

Currently, no single imaging device is capable of evaluating ocular blood flow in all of the relevant ocular tissue beds. Producing a comprehensive ocular hemodynamic evaluation therefore requires the use of several separate imaging modalities as described in this chapter. However, progress is being made to combine technologies for a more comprehensive view of ocular blood flow and metabolism. FD-OCT and retinal oximetry have added a new dimension to the study of ocular hemodynamics by incorporating measures of structure and metabolism. Kageman et al. (2007) have even shown that it is possible to measure retinal oxygen saturation using the spectral characteristics of OCT in finding significant differences in spectral absorption between blood in retinal arteries and veins. The application of these technologies may shed new light in assessing disease pathology. However, more validation studies are still needed.

Further advances toward creating reliable, reproducible measurements of blood flow and tissue oxygenation in health and disease are needed to improve our understanding of glaucomatous disease. More long-term studies of ocular perfusion pressure and blood flow in relation to the progression of OAG are needed.

## FURTHER READING

Association for Research in Vision and Ophthalmology (ARVO). Presentation entitled, 'Fourier domain optical coherence tomography blood flow assessment in patients with glaucoma: A new blood flow method'. Fort Lauderdale, FL. May 2–6, 2010.

Beach JM, Schwenzer KJ, Srinivas S et al. Oximetry of retinal vessels by dual-wavelength imaging: Calibration and influence of pigmentation. *J Appl Physiol* 1999;86:748–758.

Blum M, Bachmann K, Wintzer D et al. Noninvasive measurement of the Bayliss effect in retinal autoregulation. *Graefes Arch Clin Exp Ophthalmol* 1999;237:296–300.

Blunt MJ, Steele EJ. The blood supply of the optic nerve and chiasma in man. *J Anat* 1956;90:486–493.

Bonomi L, Marchini G, Marraffa M et al. Vascular risk factors for primary open angle glaucoma: The Egna-Neumarkt Study. *Ophthalmology* 2000;107(7):1287–1293.

Butt Z, McKillop G, O'Brien C et al. Measurement of ocular blood flow velocity using colour Doppler imaging in low tension glaucoma. *Eye* 1995;9:29–33.

Chauhan BC, Smith FM. Confocal scanning laser Doppler flowmetry: Experiments in a model flow system. *J Glaucoma* 1997;6:237–245.

Galassi F, Sodi A, Ucci F et al. Ocular hemodynamics and glaucoma prognosis: A color Doppler imaging study. *Arch Ophthalmol* 2003;121:1711–1715.

Hardarson SH, Harris A, Karlsson RA et al. Automatic retinal oximetry. *Invest Ophthalmol Vis Sci* 2006;47(11):5011–5016.

Harris A, Chung HS, Ciulla TA et al. Progress in measurement of ocular blood flow and relevance to our understanding of glaucoma and age-related macular degeneration. *Prog Retin Eye Res* 1999;18:669–687.

Harris A, Jonescu-Cuypers CP, Kagemann L et al. *Atlas of Ocular Blood Flow: Vascular Anatomy, Pathophysiology, and Metabolism*. Philadelphia: Butterworth Heinemann, 2003.

Harris A, Kagemann L, Evans DW et al. A new method for evaluating ocular blood flow in glaucoma: Pointwise flow analysis of HRF-images. *Invest Ophthalmol Vis Sci* 1997;38:439.

Hayreh SS. The central artery of the retina: Its role in the blood supply of the optic nerve. *Br J Ophthalmol* 1963;47:651–663.

Hickam JB, Frayser R. Studies of the retinal circulation in man: Observations on vessel diameter, arteriovenous oxygen difference, and mean circulation time. *Circulation* 1966;33:302–316.

Hickam JB, Sieker HO, Frayser R. Studies of retinal circulation and A-V oxygen difference in man. *Trans Am Clin Climatol Assoc* 1959;71:34–44.

Hollo G, van den Berg TJ, Greve EL. Scanning laser Doppler flowmetry in glaucoma. *Int Ophthalmol* 1996;20:63–70.

Kagemann L, Harris A, Chung HS et al. Heidelberg retinal flowmetry: Factors affecting blood flow measurement. *Br J Ophthalmol* 1998;82:131–136.

Kageman L, Wollstein G, Wojtkowski M et al. Spectral oximetry assessment with high-speed ultra-high resolution optical coherence tomography. *J Biomed Opt* 2007;12(4):041212.

Konduru RK, Tan O, Nittala MG, Huang D, Sadda SR. Reproducibility of retinal blood flow measurements derived from semi-automated Doppler OCT analysis. *Ophthalmic Surg Lasers Imaging* 2012;43(1):25–31.

Leske MC, Wu SY, Nemesure B et al. Incident open-angle glaucoma and blood pressure. *Arch Ophthalmol* 2002;120(7):954–959.

Lieberman MF, Maumenee AE, Green WR. Histologic studies of the vasculature of the anterior optic nerve. *Am J Ophthalmol* 1976;82:405–423.

Logan JF, Rankin SJ, Jackson AJ. Retinal blood flow measurements and neuroretinal rim damage in glaucoma. *Br J Ophthalmol* 2004;88:1049–1054.

Michelson G, Schmauss B. Two dimensional mapping of the perfusion of the retina and optic nerve head. *Br J Ophthalmol* 1995;79:1126–1132.

Moore D, Harris A, WuDunn D et al. Dysfunctional regulation of ocular blood flow: A risk factor for glaucoma? *Clin Ophthalmol* 2008;2(4):849–861.

Nagel E, Vilser W, Lanzl IM. Retinal vessel reaction to short-term IOP elevation in ocular hypertensive and glaucoma patients. *Eur J Ophthalmol* 2001;11:338–344.

Olafsdottir OB, Hardarson SH, Gottfredsdottir MS et al. Retinal oximetry in primary open-angle glaucoma. *Investigative Ophthalmology & Visual Science* 2011;52(9):6409–6413.

Olver JM, Spalton DJ, McCartney AC. Microvascular study of the retrolaminar optic nerve in man: The possible significance in anterior ischaemic optic neuropathy. *Eye* 1990;4:7–24.

Petrig BL, Riva CE, Hayreh SS. Laser Doppler flowmetry and optic nerve head blood flow. *Am J Ophthalmol* 1999;127:413–425.

Quaranta L, Manni G, Donato F et al. The effect of increased intraocular pressure on pulsatile ocular blood flow in low tension glaucoma. *Surv Ophthalmol* 1994;38(Suppl):S177–S181.

Quigley HA, West SK, Rodriguez J et al. The prevalence of glaucoma in a population-based study of Hispanic subjects: Proyecto VER. *Arch Opthalmol* 2001;119(12):1819–1826.

Scheider A. Indocyanine green angiography with an infrared scanning laser ophthalmoscope. Initial clinical experiences. *Ophthalmologe* 1992;89:27–33.

Schumann J, Orgul S, Gugleta K et al. Interocular difference in progression of glaucoma correlates with interocular differences in retrobulbar circulation. *Am J Ophthalmol* 2000;129:728–733.

Silver DM, Farrell RA, Langham ME et al. Estimation of pulsatile ocular blood flow from intraocular pressure. *Acta Ophthalmol (Suppl)* 1989;191:25–29.

Tielsch JM, Katz J, Sommer A et al. Hypertension, perfusion pressure, and primary open-angle glaucoma. A population-based assessment. *Arch Ophthalmol* 1995;113(6):216–221.

Trew DR, Smith SE. Postural studies in pulsatile ocular blood flow: II. Chronic open angle glaucoma. *Br J Ophthalmol* 1991;75:71–75.

Wagemann A, Salzmann P. Anatomische Untersuchungen uber einseitige Retinitis Haemorrhagica mit Secundar-Glaucom nebst Mittheilungen uber dabei beobachtete Hypopyon-Keratitis. *Arch Ophthalmol* 1892;38:213.

Wang Y, Bower BA, Izatt JA et al. Retinal blood flow measurement by circumpapillary Fourier domain Doppler optical coherence tomography. *J Biomed Opt* 2008;13(6):064003.

Wang Y, Fawzi AA, Varma R, Sadun AA, Zhang X, Tan O, Izatt JA, Huang D. Pilot study of optical coherence tomography measurement of retinal blood flow in retinal and optic nerve diseases. *Invest Ophthalmol Vis Sci* 2011;52(2):840–845.

Wang Y, Lu A, Gil-Flamer J et al. Measurement of total blood flow in the normal human retina using Doppler Fourier-domain optical coherence tomography. *Br J Ophthalmol* 2009;93(5):634–637.

Weinreb RN, Harris A. *Ocular Blood Flow in Glaucoma: The 6th Consensus Report of the World Glaucoma Association*. Amsterdam, the Netherlands: Kugler Publications, 2009.

Williamson TH, Harris A. Color Doppler ultrasound imaging of the eye and orbit. *Surv Ophthalmol* 1996;40(4):255–267.

Williamson TH, Harris A. Ocular blood flow measurement. *Br J Ophthalmol* 1994;78:939–945.

Yap MK, Brown B. The repeatability of the noninvasive blue field entoptic phenomenon method for measuring macular capillary blood flow. *Optom Vis Sci* 1994;71:346–349.